Universidad San Francisco de Quito USFQ

Colegio de Ciencias e Ingenierías

Two-dimensional lagrangian model for nonlinear soil-structure interactions

Artículo académico

Juan Martin Cadena Proaño

Ingeniería Civil

Trabajo de titulación presentado como requisito para la obtención del título de Ingeníero Civil

Quito, 21 de diciembre 2017

UNIVERSIDAD SAN FRANCISCO DE QUITO

COLEGIO DE CIENCIAS E INGENIERÍAS

HOJA DE CALIFICACIÓN DE TRABAJO DE TITULACIÓN

A two-dimensional lagrangian model for nonlinear soil-structure interactions

Juan Martin Cadena Proaño

Ingeniería Civil

Calificación:

Nombre del Profesor: Ing. Alex X. Jerves Mg., M.Sc., PhD

_____

Quito, 21 de diciembre de 2017

Derechos de Autor

Por medio del presente documento certifico que he leído todas las Políticas y Manuales de la Universidad San Francisco de Quito USFQ, incluyendo la Política de Propiedad Intelectual USFQ, y estoy de acuerdo con su contenido, por lo que los derechos de propiedad intelectual del presente trabajo quedan sujetos a lo dispuesto en esas Políticas. Asimismo, autorizo a la USFQ para que realice la digitalización y publicación de este trabajo en el repositorio virtual, de conformidad a lo dispuesto en el Art. 144 de la Ley Orgánica de Educación Superior.

Firma: _____

Nombres y apellidos   Juan Martin Cadena Proaño

Codigo: 00114203

Cedula de identidad: 17200725500

Lugar y fecha: Quito, 21 de diciembre de 2017

Abstract

We introduce a two-dimensional lagrangian model to determine nonlinear soil-structure interactions (NL-SSI) and behavior of a three-story building when subjected to a seismic excitation. While most models tackle linear soil-structure interactions (SSI) through finite element analysis (FEM), here we propose a finite difference method (FDM) to determine NL-SSI. First, a lagrangian framework is used to derive the equations of motion of the soil-building system for any given vibrational excitation. Second, the equations of motion are discretized by means of forward and central finite difference schemes. Third, a classical Newton - Raphson (NR) approach is carried out in order to solve the non-linear system of algebraic equations obtained from the FD discretization. Fourth, the equations of motion were linearized to implement a modal and frequency analysis of the proposed system. Four benchmark problems are solved in order to test the aforementioned approach. The first three examples consist of an initial value problem (IVP) were displacements and velocities are prescribed without an external force. Finally, the last problem includes external forcing of the same building subjected to a real seismic register.

Resumen

Presentamos un modelo lagrangiano bidimensional para determinar las interacciones no lineales de la estructura junto suelo (ISE-NL) y el comportamiento de un edificio de tres pisos cuando se somete a una excitacin sísmica y un registro real. Si bien la mayora de los modelos abordan las interacciones lineales suelo-estructura (SSI) a través del análisis de elementos finitos (MEF), se propone un método de diferencias finitas (FDM) para determinar ISE-NL. Primero, se usa un marco de mecánica lagrangiana para derivar las ecuaciones de movimiento del sistema de suelo y estructura para cualquier excitacin vibratoria dada. En segundo lugar, las ecuaciones de movimiento se discretizan mediante diferencias finitas delanteras y centrales. En tercer lugar, se lleva a cabo un Newton - Raphson (NR) clásico para resolver el sistema no lineal de ecuaciones algebraicas obtenidas a partir de la discretización de diferencias finitas. En cuarto lugar, las ecuaciones de movimiento se linealizaron para implementar un análisis modal y de frecuencia del sistema propuesto. Se resuelven cuatro problemas para probar el enfoque mencionado anteriormente. Los primeros tres ejemplos consisten en problemas de valor inicial (IVP) donde los desplazamientos y las velocidades se prescriben sin forzamiento externo. Finalmente, el último problema incluye el forzamiento externo del mismo edificio sometido a un registro sísmico real.

Palabras clave: interaccion suelo estructura; no lineal; diferencias finitas; dos dimensiones; registro sísmico

A two-dimensional lagrangian model for nonlinear soil-structure interactions

Juan M. Cadena & Alex X. Jerves*

College of Science & Engineering, Universidad San Francisco de Quito, Quito Pichincha 1712841 Ecuador

1   Introduction

Seismic numerical modeling is a recent field where the increasing computational power of the last decades has been crucial for the development of structural-dynamic analysis [1, 2]. One-dimensional analyses, so-called 'stick-models', have fallen short in the adequate prediction of structural behavior to seismic excitation [3]. In fact, the main drawback is that the structural bases are considered as infinitely rigid plates, i.e., the effects of the SSI are completely omitted, which in many cases might be inappropriate.

It is at the end of the decade of the 70s when scientists began to put greater emphasis in SSI. Supported mainly by the appearance of the first computers, authors like Chopra [4] and Richart[5] began to develop numerical methods to model the seismic behavior of the structures [6–8].

These methods, used even today, subdivide the structure and the soil, which leads to a separate analysis of their behavior. The soil is modeled as a continuous medium and is therefore analyzed by means of finite elements, while the structure is modeled by classic methods, for instance, 'stick-models'. [9].

On the other hand, an early SSI model through the use of FDM was developed by Agabein [10]. Dashpots were used in order to model the structure, as well as the soil. However, although powerful, this method was displaced by the FEM methods previously specified, mainly, because of geometry and constituve models limitations [9].

Even if previously proposed models have been able to capture quite well the effects of nonlinear deformations produced by SSI in the soil by means of finite element or finite difference methods, these are usually not able to describe the nonlinear movement of the structure. The proposed

*Corresponding author. E-mail: ajerves@usfq.edu.ec (Alex X. Jerves)

model beyond its numerical solution form, i.e. by means of FEM or FDM, proposes to study the nonlinear physical motion of a structure caused by a seismic excitation.

This is possible through the use of Lagrangian mechanics, which allow to overcome the limitations of Newtonian mechanics when studying nonlinear dynamic behaviors [11]. After obtaining the ordinary differential equations of the movement of the structure, a numerical approach was used to solve them. First, by discretizing the *system of ordinary differential equations* (ODE) via *finite difference* and then by solving the resulting nonlinear system of algebraic equations with a classical local *Newton-Raphson method*.

2   Soil-structure system and constitutive assumptions

The system proposed to model the behavior and interaction of the three-story structure with the soil is located in a two-dimensional space. The structure consists of a two story building seated on a mat foundation, which is subjected to a seismic excitation, as described in Figure 1. The seismic response is approached as an IVP, in which both the speed and the initial position are prescribed in order to mimic the effect of ground acceleration.
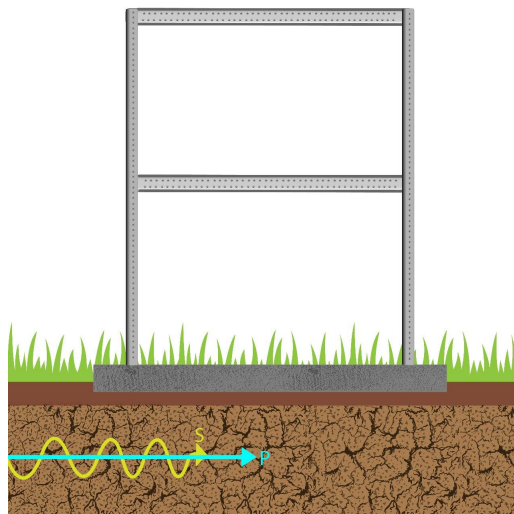

Figure 1:   Steel building structure in two-dimensions undergoing a seismic event.

Soil behavior was modeled taking into consideration previous research, especially by authors such as Gazetas, Dorby, Roesset, and Wolf, who proposed to model the behavior of the foundations as a system of a single degree of freedom idealized by means of a spring and a dashpot [12–16]. As

depicted in Figure 2, the proposed model takes into account the physical response of the surface mat foundation, that is in direct contact with the ground, which constitutes a substructure by itself, i.e., the soil is represented by a mass-spring-dashpot model. [17].
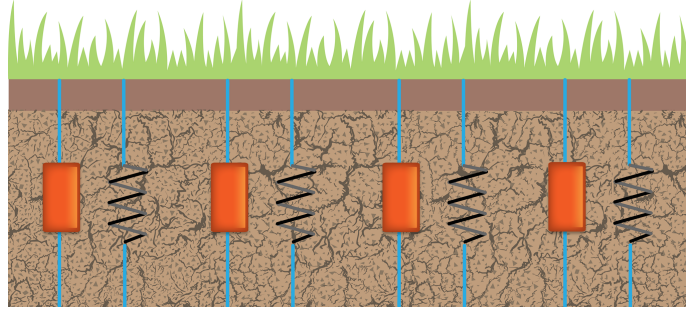

Figure 2: Soil constitutive model consisting of linear springs and dashpots.

Furthermore, to simulate the dissipative capacity of the structure itself, two dashpots were used, in the same manner as we modeled the behavior of the soil. It is important to note that the mass of each of the floors was concentrated in a single point as presented in Figure 3.
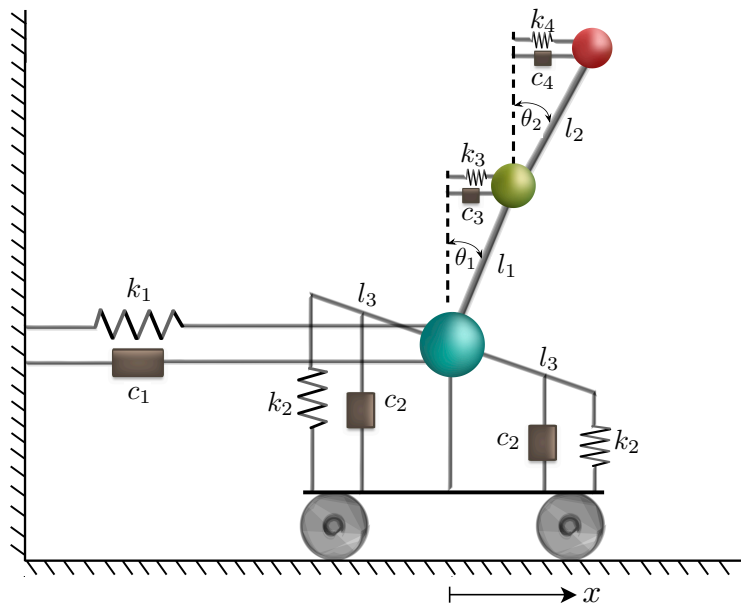

Figure 3: Two-dimensional soil-structure model.

3 Lagrangian model

Due to the complexity of the proposed model, in which the use of dashpots and springs to model the dissipation of energy is present in all the elements of the system, the formulation of the behavior of the structure through Newtonian mechanics can become extremely tedious [18]. Therefore, the energy-based framework of lagrangian mechanics was used in order to obtain the equations describing the position of the structure [19].

Let us introduce the *lagrangian*, $\mathcal{L} = T - V$, where T represents the total kinetic energy of the system, while V stands for the potential energy of the system [20]. Therefore, by the *Principle of Stationary Action* that takes by argument the *lagrangian* [11],

$$S[\boldsymbol{q}] = \int_{t_i}^{t_f} L(\boldsymbol{q}, \dot{\boldsymbol{q}}; t) \, dt$$

where $\boldsymbol{q}(t)$ represents the path of action from instant t_i to t_f. From which, we can formulate the *Euler-Lagrange* equations by means of variational calculus. In our model, these will form a system of three equations regarding each degree of freedom (DOF) of the structure [20],

$$\frac{\partial \mathcal{L}}{\partial \theta_1} = \frac{d}{dt}\left(\frac{\partial \mathcal{L}}{\partial \dot{\theta}_1}\right), \quad \frac{\partial \mathcal{L}}{\partial \theta_2} = \frac{d}{dt}\left(\frac{\partial \mathcal{L}}{\partial \dot{\theta}_2}\right) \quad \text{and} \quad \frac{\partial \mathcal{L}}{\partial x} = \frac{d}{dt}\left(\frac{\partial \mathcal{L}}{\partial \dot{x}}\right)$$

The potential energy is given by:

$$\begin{aligned} V =& \frac{1}{2}k_1 x^2 + \frac{1}{2}k_3 L_1^2 \sin^2\theta_1 + \frac{1}{2}k_4 \left(L_2 \sin\theta_2\right)^2 + L_1 \cos\theta_1 m_1 g + m_2 g \left(L_2 \cos\theta_2 + L_1 \cos\theta_1\right) \\ &+ k_2 L_3^2 \sin^2\theta_1 \end{aligned} \tag{1}$$

while the kinetic energy,

$$\begin{aligned} T =& \frac{1}{2}m_0 \dot{x}^2 + \frac{1}{2}m_1 \left[l_1^2 \dot{\theta}_1^{\,2} \sin^2(\theta_1) + \left(l_1 \dot{\theta}_1 \cos(\theta_1) + \dot{x}\right)^2\right] \\ &+ \frac{1}{2}m_1 \left[l_1^2 \dot{\theta}_1^{\,2} \sin^2(\theta_1) + \left(l_1 \dot{\theta}_1 \cos(\theta_1) + \dot{x}\right)^2\right] \\ &+ \frac{1}{2}m_2 \left[\left(2l_1 \dot{\theta}_1 \sin(\theta_1) + l_2 \dot{\theta}_2 \sin(\theta_2)\right)^2 + \left(2l_1 \dot{\theta}_1 \cos(\theta_1) + l_2 \dot{\theta}_2 \cos(\theta_2) + \dot{x}\right)^2\right] \end{aligned} \tag{2}$$

Hence, we arrive to the following system nonlinear differential equations:

$$
\begin{cases}
c_3 l_1 \dot{\theta}_1 \cos(\theta_1) + 2 c_2 l_3 \dot{\theta}_1 \cos(\theta_1) + c_3 \dot{x} - g l_1 m_1 \sin(\theta_1) - g l_1 m_2 \sin(\theta_1) \\[2mm]
+ \dfrac{1}{2} k_3 l_1^2 \sin(2\theta_1(t)) + k_2 l_3^2 \sin(2\theta_1) + 2 l_2 l_1 m_2 \dot{\theta}_2{}^2 \sin(\theta_1 - \theta_2(t)) + l_1^2 m_1 \ddot{\theta}_1 + 4 l_1^2 m_2 \ddot{\theta}_1 \\[2mm]
+ 2 l_2 l_1 m_2 \ddot{\theta}_2 \cos(\theta_1 - \theta_2) + l_1 m_1 \cos(\theta_1) \ddot{x} + 2 l_1 m_2 \cos(\theta_1) \ddot{x} = 0 \hfill (3) \\[6mm]

l_2 \left[c_4 \dot{\theta}_2 \cos(\theta_2) + m_2 \left(-g \sin(\theta_2) + 2 l_1 \left(\dot{\theta}_1 \cos(\theta_1 - \theta_2) - \dot{\theta}_1{}^2 \sin(\theta_1 - \theta_2) \right) + \cos(\theta_2) \ddot{x} \right) \right] \\[2mm]
+ c_4 \left(2 l_1 \dot{\theta}_1 \cos(\theta_1) + \dot{x} \right) + \dfrac{1}{2} k_4 l_2^2 \sin(2\theta_2) + l_2^2 m_2 \ddot{\theta}_2 = 0 \hfill (4) \\[6mm]

c_1 \dot{x} + k_1 x + m_1 \left[l_1 \left(\ddot{\theta}_1 \cos(\theta_1) - \dot{\theta}_1{}^2 \sin(\theta_1) \right) + \ddot{x} \right] + m_2 \left[l_1 \left(2 \ddot{\theta}_1 \cos(\theta_1) - 2 \dot{\theta}_1{}^2 \sin(\theta_1) \right) \right. \\[2mm]
\left. + l_2 \left(\ddot{\theta}_2 \cos(\theta_2) - \dot{\theta}_2{}^2 \sin(\theta_2) \right) + \ddot{x} \right] + m_0 \ddot{x} = 0 \hfill (5)
\end{cases}
$$

As discussed earlier, this is an IVP, where for $t = 0$ both the position and speed of the system are given [21]. However, we deal with a system of highly nonlinear ordinary differential equations (see, Equations (3), (4) and (5)), which can not be solved simply as in a linear system. The proposed method for solving the system of differential equations is a combination of a finite difference discretization scheme and the NR method. [22, 23].

4 Finite difference discretization

The finite difference scheme to be used is *forward Euler* for the first derivatives and a second order central finite difference for the higher order derivatives, which is a simple yet powerful approach for the solution of IVPs [23, 24]. It is a *multi-step explicit method* in which the system state x^{n+1} is given by previous values x^n and x^{n-1}.

$$
D_+ x = \frac{x^{n+1} - x^{n-1}}{2 \Delta t}, \quad n = 0, 1, 2... \tag{6}
$$

$$
D^2 x = \frac{x^{n+1} - 2 x^n + x^{n-1}}{\Delta t^2}, \quad n = 0, 1, 2... \tag{7}
$$

However, as expected, the discretization of the ODEs results in a nonlinear algebraic equation system, which is impossible to solve by classical methods for linear equations such as Gaussian Elimination or LU factorization [25]. Refer to Appendix for a glimpse at how Equation (3), (4) and (5) look once discretized.

Taking into account that this is a multi-step explicit finite difference scheme and an IVP, the initial conditions are given in $t = 0$, i.e., when $n = 0$. To calculate the state of the system when $n = 1$ we use a forward Euler approximation as detailed above [26].

5 Solution of the discretized model

To attack the equations we used a multivariable *local* NR to find numerical approximations of the roots of a system of equations [27]. The iterative process is given by [28],

$$x_{k+1} = x_k - J(x_k)^- f(x_k)$$

where $J_{ij} = \dfrac{\partial f_i}{\partial x_j}$ represents the *Jacobian* of the system of nonlinear equations.

The NR used is locally convergent, meaning that the initial iteration x^0 has to be close to the actual solution in order to find convergence [28, 29]. That is why within the solution scheme it is proposed that for time x^n the initial iteration is given by the roots, x^{n+1}, found approximated in the previous iteration of the time discretization . It is in this way that we ensure a correct and reasonable convergence of the method [24, 28].

As mentioned in [28] the convergence of the local NR is given by,

$$||\mathbf{R}_{k+1}|| \le c\,||\mathbf{R}_k||^2 \tag{8}$$

for $c > 0$.

The convergence described in 8 is quadratic, therefore, the residue of the present iteration doubles that of the next iteration.

5.1 Proposed algorithm

function LAGRANGIANMODELING$(J, f, x^0, tol, \Delta t)$

    Evaluate x^1 using *forward Euler* finite difference, see, Equation (6).

    for n : 1 to T **do**

        $k = 1$

        while $||\mathbf{R}|| > tol$ **do**

            $x_k^{n+1} \leftarrow x_k^n - J_k(x^n)^- f_k(x^n)$

            $\mathbf{R} = f_k / f_1$

            $k \leftarrow k + 1$

        end while

    end for

end function

6 Linearized model and modal analysis

Now we are going to linearize the proposed model, in other words to assume small displacements for the response of the building due to the seismic excitation. Therefore, $\sin(\theta_1) = \theta_1$ and $\cos(\theta_1) = 1$, while $\dot{\theta}_1^2 \approx 0$ as we expect infinitesimal changes for the angular displacements in time. The same assumptions were made for θ_2.

Also, we assumed the same longitudes and masses for the whole system, the same stiffness for the stories of the building (K_1), and a general stiffness for the soil (K_2). The dissipation constants were canceled, as modal analysis is made only in function of the geometry and materials of the system. Finally, we arrive to the following system of linear differential equations.

$$m \underbrace{\begin{pmatrix} 5L_1^2 & 2L_1^2 & 3L_1 \\ 2L_1^2 & L_1^2 & L_1 \\ 3L_1^2 & L_1 & 3 \end{pmatrix}}_{M} \begin{Bmatrix} \ddot{\theta}_1 \\ \ddot{\theta}_2 \\ \ddot{x} \end{Bmatrix} + \underbrace{\begin{pmatrix} 2k_2 L_2^2 + L_1(k_1 L_1 - 2gm) & 0 & 0 \\ 0 & -L_1(gm - k_1 L_1) & 0 \\ 0 & 0 & k_2 \end{pmatrix}}_{K} \begin{Bmatrix} \theta_1 \\ \theta_2 \\ x \end{Bmatrix} = \begin{Bmatrix} 0 \\ 0 \\ 0 \end{Bmatrix}$$

$$(9)$$

Where in order to find the vibrational modes of the linearized soil-structure system the following eigenvalue problem has to be tackled.

$$\left(K - \omega^2 M\right) \eta e^{i\omega t} = 0 \implies \det(K - w^2 M) = 0$$

which for the proposed model yields three modes (η_1, η_2, η_3), complying with the three degrees of freedom that govern system movement.

7   Numerical examples

In this section, we solved four benchmark problems based on a three story steel moment frame building seated on a surface mat foundation. The soil-structure system and its constitutive parameters are shown by Figure 4,
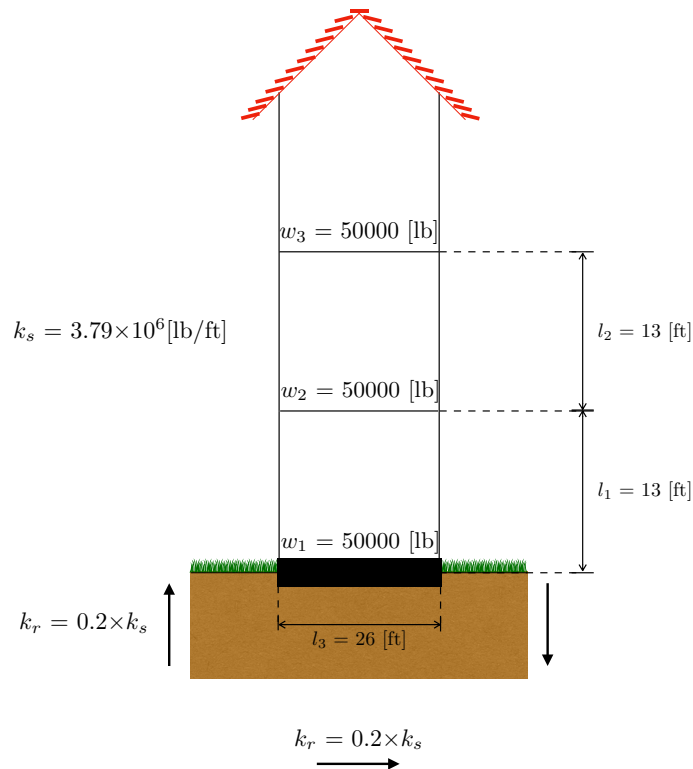
Figure 4:   Three story steel moment frame building seated on a surface mat foundation, and its corresponding constitutive parameters, used to solve the four benchmark problems herein proposed.

The dissipation constants for soil and structure (c_s,c_r,c_h) were obtained as percentages of the critical dumping of each section of the model. For instance, for the structure

$$c_s = 2\xi_c m_1 \sqrt{\frac{k}{m}}$$

where, ξ_s represents a percentage of dissipation with respect the critical dumping. Thus, for the steel moment frame structure we used $\xi_s = 2\%$, while for the soil rotational and horizontal dissipations we assumed $\xi = 10\%$.

For the constitutive values of the springs, they were computed taking into consideration equivalent displacement stiffness for two fixed columns, that is

$$k_s = \frac{24 E_s I_s}{l^3}$$

where for calculating the inertia of the section, it was considered to have typical values for a steel rectangular hollow column, of $I_s = 0.085\, ft^4$. On the other hand, the stiffness of the soil was estimated to be a 20% of one of the structure.

The acceleration and velocity records shown by Figure 5 were obtained from the Pedernales station located at latitud 0.068, longitude -80.057, 2016 N-S component, Muisne earthquake in Ecuador [30]. The magnitude of the event was of 7.8 on the moment magnitud scale at 27 Km depth [31]. The raw data of the acceleration record was processed using PRISM, which is a software for analyzing acceleration time series to produce compatible velocity and displacement records. The signal of the acceleration record was corrected and integrated in order to obtain the velocity record [32], shown in Figure 5.
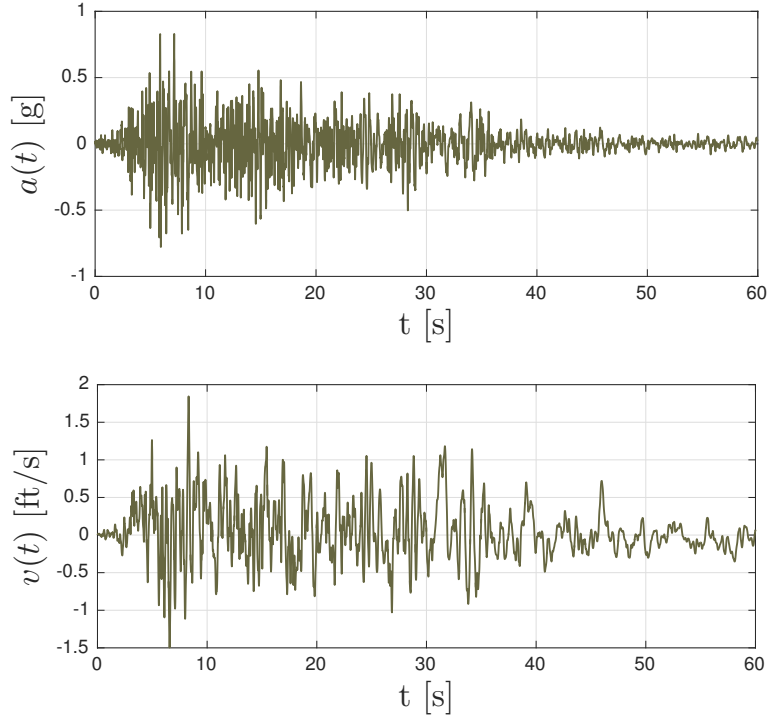
Figure 5: Acceleration and velocity registers form 2016 Muisne, Ecuador, earthquake, M 7.8 at 27 Km depth.

We proposed three IVP's, where the position and velocity at $t = 0\,s$ were prescribed. These conditions were obtained by using the seismic record depicted by Figure 5, from which the maximum velocity and displacement values (see, Table 1) were computed and then used as initial conditions for the proposed problems.

Problem	x(0)	v(0)
1	3.27 ft	0
2	0	1.84 ft/s
3	3.27 ft	1.84 ft/s

Table 1: Initial conditions for the first three benchmark problems proposed.

7.1 Benchmark problem No. 1

In this first IVP we prescribe a position of $x(0) = 3.27 ft$, as can be seen from Table 1. Figures 6 and 7 show the response of the system.
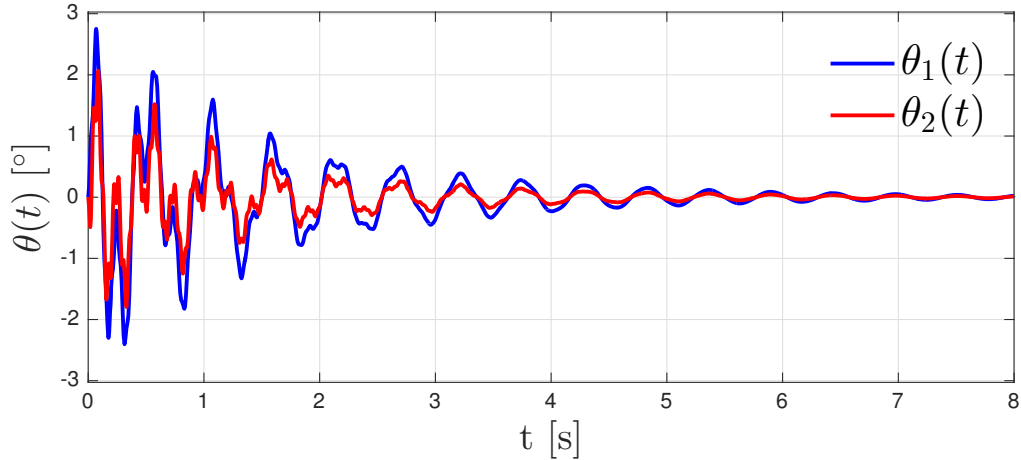
10

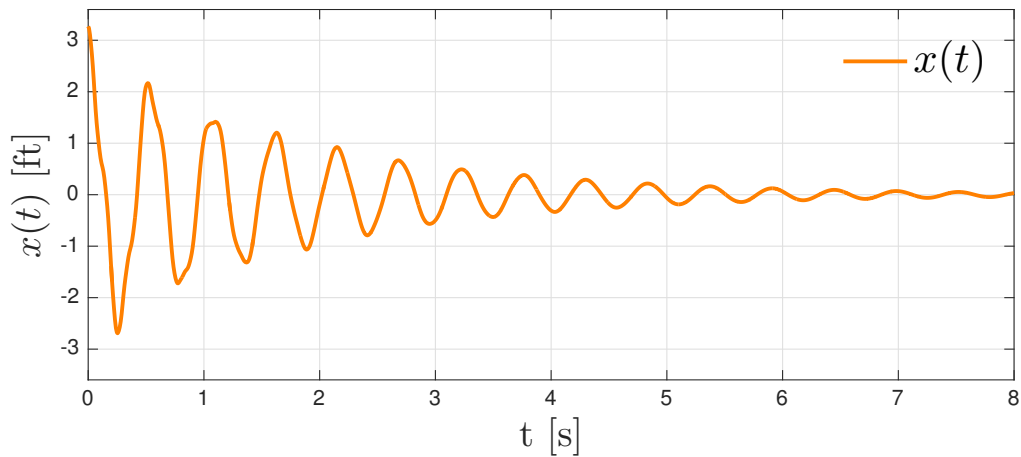Figure 6: Evolution of θ_1 and θ_2 for benchmark problem No. 1.

Figure 7: Evolution of x for benchmark problem No. 1.

Since damping is a natural feature of multistory structures and soil, and also present in our model, the energy pumped into the system once the initial conditions are applied is dissipated. As expected, the decay rate shown by Figures 6 and 7, resembles the one of a positive undercritically-damped system undergoing free vibrations, mainly because damping values where picked taking into consideration the fact that common buildings behave in this way. Recall that we used damping values as a percentage of the critical damping of the model, that is, 2% for the steel structure and 10% for the soil. The system stops completely after 8 seconds of free vibrations for all its DOF.

On the other hand, the DOF of the structure, θ_1 and θ_2 (see, Figure 6), yield almost 3°, which in terms of deformational analysis it can be considered high enough to induce nonlinear behavior

11

in the system. Thus, from Figures 6 and 7, it is worth noticing that these angular displacements are directly influenced by the inclusion of the soil as a part of the model. Contrary to classic "stick-models" where the interaction with the soil is neglected by assuming it to be infinitely rigid, our model, that considers soil deformation, takes into account the "softening" of the structure's behavior. Hence, the importance of including the soil as a fundamental part of the analysis, which, in turn, can induce the structure into nonlinear behavior. Therefore the relevance as well as usefulness, for these type of problems, of considering nonlinearity coming either from the geometry or the constituve behavior of the system.

Finally, since nonlinear deformations have been considered as part of the model (see, Section 3), a NR method has to be used in order to solve the discretized nonlinear system given by Equations (3), (4) and (5). The convergence of the NR used to solve the aforementioned system of equations is depicted by Figure 8 at different time steps. It is important to mention that tolerance is reached at the first iteration, mainly because of the quality of the first guess given to initialize the NR, the small size of the time steps, as well as the high stiffness given to the structure and soil that keep the system's behavior close to linearity. For the first three benchmark problems we used a time step $\Delta t = 1 \times 10^{-5}$.
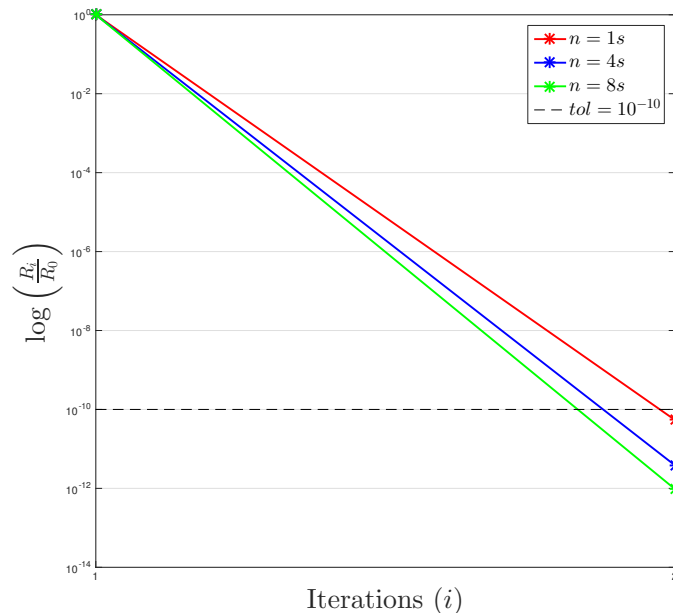

Figure 8: NR convergence at different time steps: $n =$ 1 s, 4 s and 8 s, for a tolerance of 1×10^{-10}, and for benchmark problem No. 1.

12

7.2 Benchmark problem No. 2

In this second benchmark problem we prescribe a velocity of $v(0) = 1.84ft/s$, as can be seen from Table 1. In this case, Figures 9 and 10 show the response of the system.
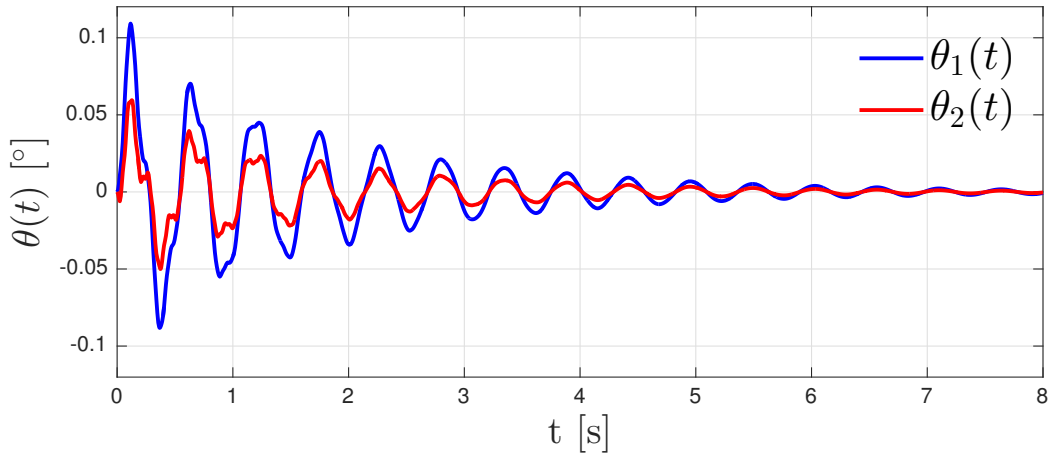

Figure 9:   Evolution of θ_1 and θ_2 for benchmark problem No. 2.
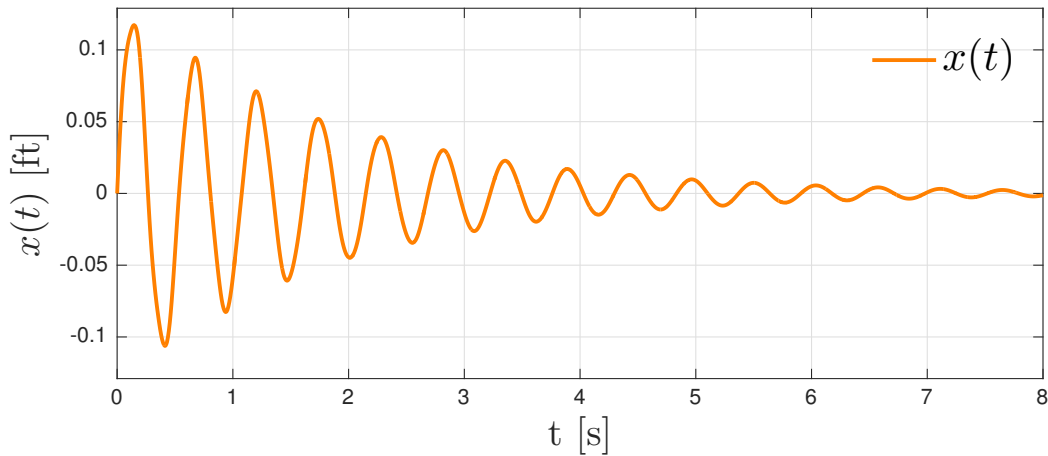

Figure 10:   Evolution of x for benchmark problem No. 2.

The behavior of the model shown in Figures 9 and 10 resembles the one analyzed for benchmark problem No. 1. Once again, the structure stops around 8 seconds of free motion and the decay rate is exponential as expected. However, in this example, the behavior of the system is much more linear than for benchmark problem No. 1. In this case, θ_1 and θ_2 (see, Figure 9), yield less than 0.15°, which in terms of deformational analysis, it can be considered small enough to be linear.

Since linearity is predominant for this benchmark problem a one iteration convergence is also expected for the NR method (see, Figure 11).
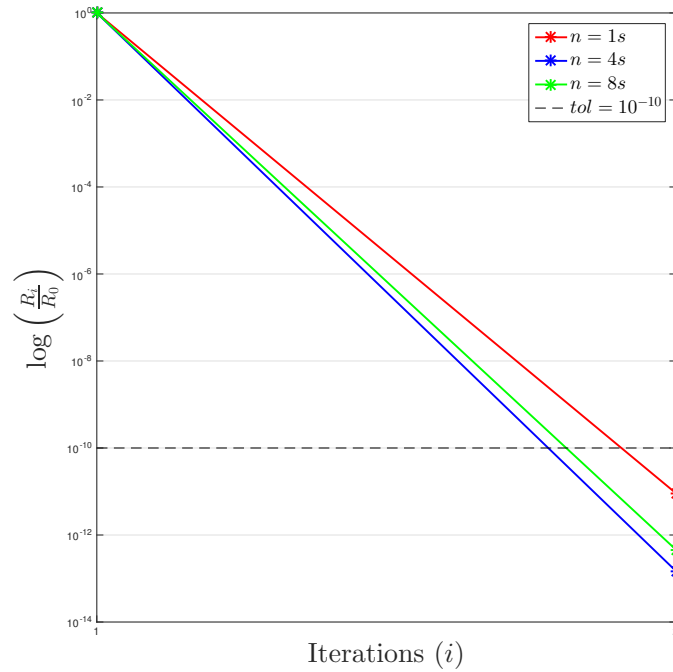

Figure 11: NR convergence at different time steps: $n = 1$ s, 4 s and 8 s, for a tolerance of 1×10^{-10}, and for benchmark problem No. 2.

7.3 Benchmark problem No. 3

For our third IVP we prescribe a velocity of $v(0) = 1.84 ft/s$ and a position of $x(0) = 3.27 ft$ (a combination of two the former benchmark problems), as can be seen from Table 1. Figures 12 and 13 illustrate the response of the system.
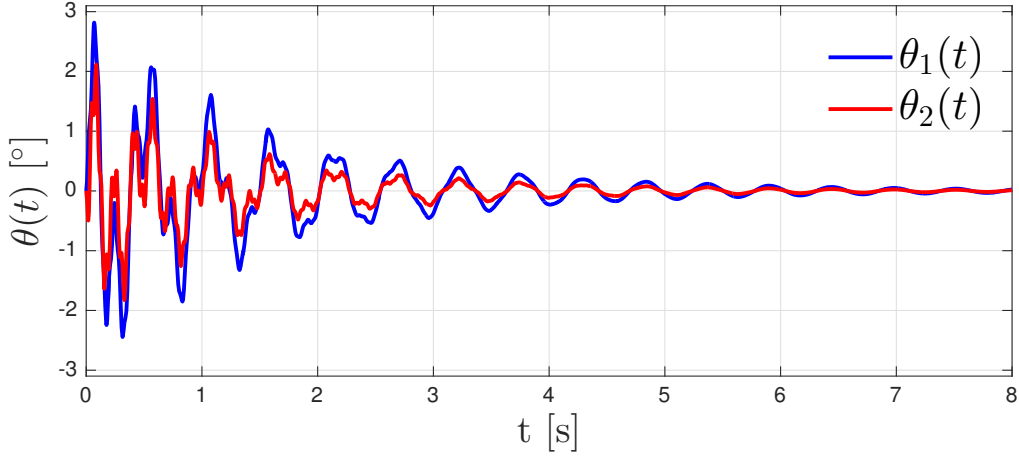
Figure 12: Evolution of θ_1 and θ_2 for benchmark problem No. 3.
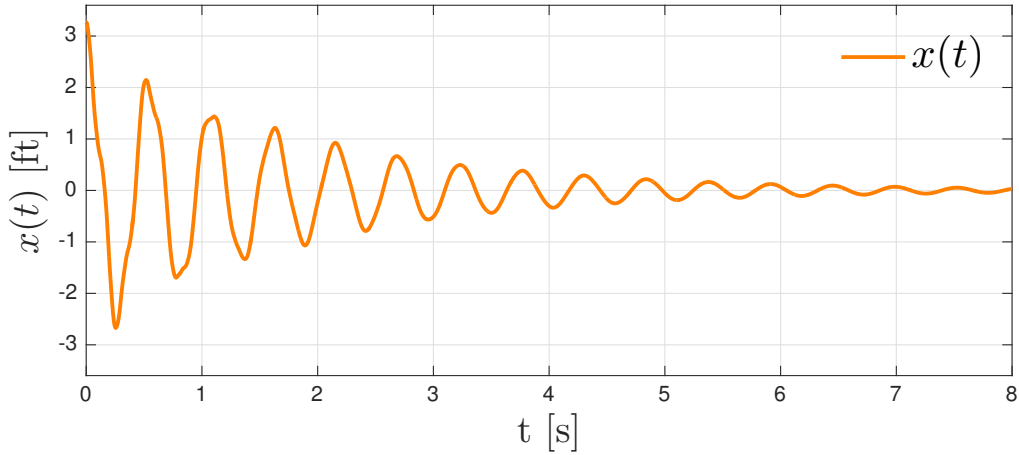

Figure 13: Evolution of x for benchmark problem No. 3.

For this IVP the behavior shown by Figures 12 and 13 resembles the one analyzed for the first and second benchmark problems. The structure reaches stop at around 8 seconds of free vibrations and the decay rate is exponential as expected. Furthermore, from this combination of benchmark problem No. 1 and No. 2, it can be seen that the predominant behavior is dictated by the prescribed initial displacement rather than the prescribed initial velocity whose effect, in this case, can be considered as structural noise, and therefore negligible.

Provided that the prescribed initial displacement governs the physics of the entire problem, the NR once again is expected to converge at the first iteration (see, Figure 14).
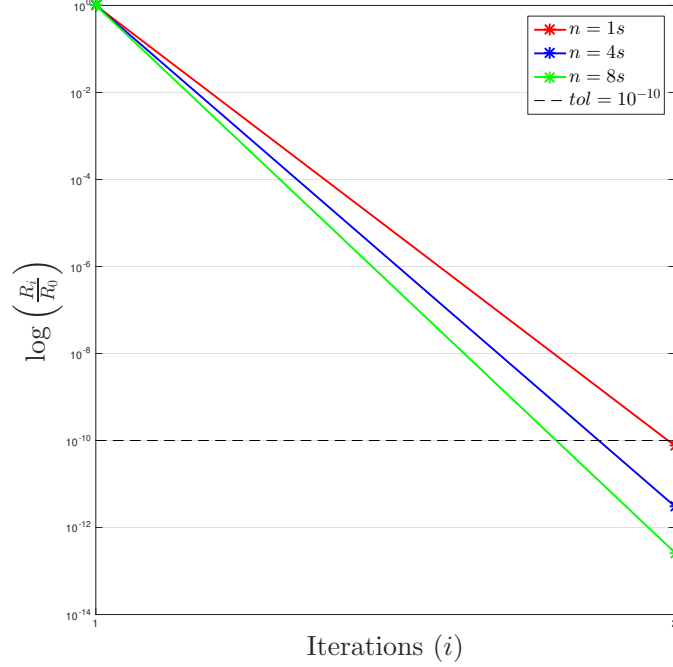
Figure 14: NR convergence at different time steps: $n = 1$ s, 4 s and 8 s, for a tolerance of 1×10^{-10}, and for benchmark problem No. 3.

7.4 Real seismic excitation response

In this last example, the system undergoes external forcing given by a real seismic acceleration record (see, Figure 5). The acceleration is applied at the base of the structure, i.e., the bottom mass that in our model represents the surface mat foundation of the building. In order to properly add the seismic record to the motion equations, the acceleration time series is multiplied by the total mass of the building ($M_t = m_0 + m_1 + m_2$; see, Figure 4) and then added to the right hand side of Equation (5), from where we arrive to

$$
c_1 \dot{x} + k_1 x + m_1 \left[l_1 \left(\ddot{\theta}_1 \cos(\theta_1) - \dot{\theta}_1^2 \sin(\theta_1) \right) + \ddot{x} \right] + m_2 \left[l_1 \left(2\ddot{\theta}_1 \cos(\theta_1) - 2\dot{\theta}_1^2 \sin(\theta_1) \right) \right.
$$
$$
\left. + l_2 \left(\ddot{\theta}_2 \cos(\theta_2) - \dot{\theta}_2^2 \sin(\theta_2) \right) + \ddot{x} \right] + m_0 \ddot{x} = M_T a(t)
$$

On the other hand, Equations (3) and (4) stay the same, as forcing caused by the acceleration record is only applied to the base of the structure. Finally, the behavior of the soil-structure system

16

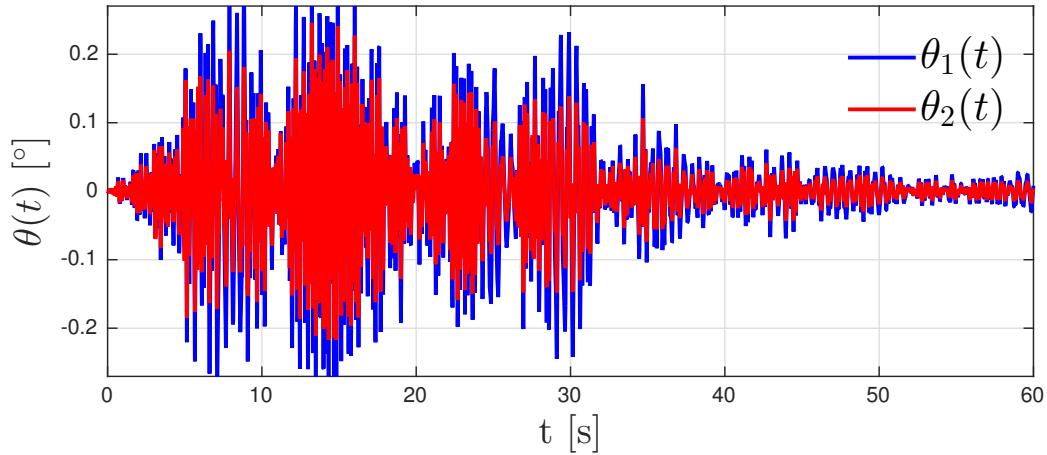when undergoing a real seismic excitation is shown by Figures 15 and 16.

Figure 15: Evolution of θ_1 and θ_2 for a real seismic excitation.
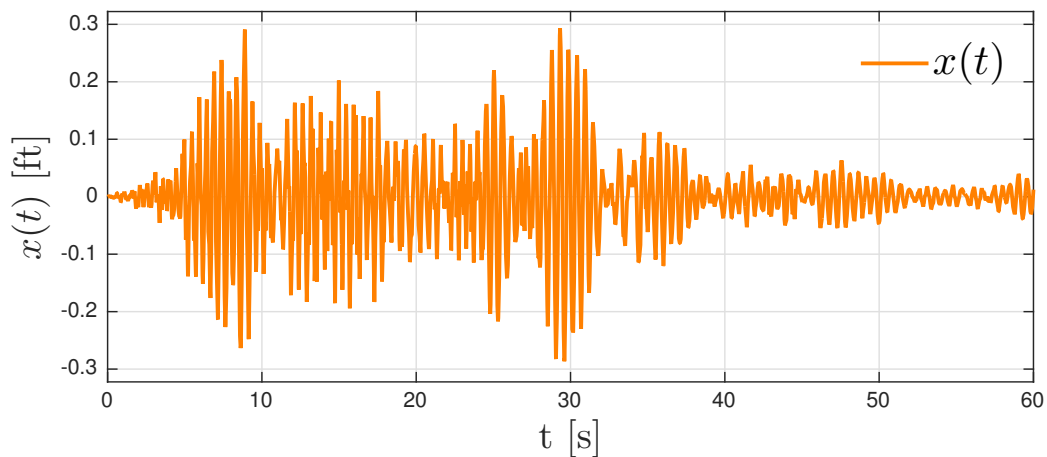
Figure 16: Evolution of x for a real seismic excitation.

Table 2 summarizes the average and maximum values corresponding to the angular and horizontal displacements of the system. As can be inferred from the table in mention, the structure behaves in a much linear way than the former cases with angles of less than 0.35°. In contrast with this, the displacements for the base of the structure is the most nonlinear among the three DOF with values of less than 0.3 ft.

DOF	Average	Maximum
θ_1	0.0519°	0.3208°
θ_2	0.0354°	0.2463°
x	0.0492 ft	0.2930 ft

Table 2: Average and maximum angular and horizontal displacements for a real seismic excitation.

These results correspond to the acceleration record shown in Figure 5 as well as the values of stiffness and damping previously assigned to the soil in our benchmark problem. Furthermore, these values do not correspond to the actual soil constituve properties for the place (Pedernales station located at latitud 0.068, longitude -80.057). More experimental testing is needed in order to find the real values of stiffness and damping of the soil at the aforementioned place, which in turn, may have a significant impact on the final behavior of the structure. Bear in mind that the current analysis was done for a seismic event of magnitud $M_w = 7.8$ and that this might be much greater, for instance, the seismic event in Chile, 2010 with a magnitude on the moment scale of 8.8 [33]. While for the structural and soil features used in this case the nonlinear analysis could not be as relevant since the angular displacements are considerably small. It might not be the case when geometry, seismic intensity and soil properties are different, not to mention the quality of the materials and construction of the structure itself.

As already mentioned in the last paragraph, the physical behavior of the current benchmark problem tends to linearity. Thus, the NR is expected, once again, to converge at the first iteration, as shown by Figure 17.
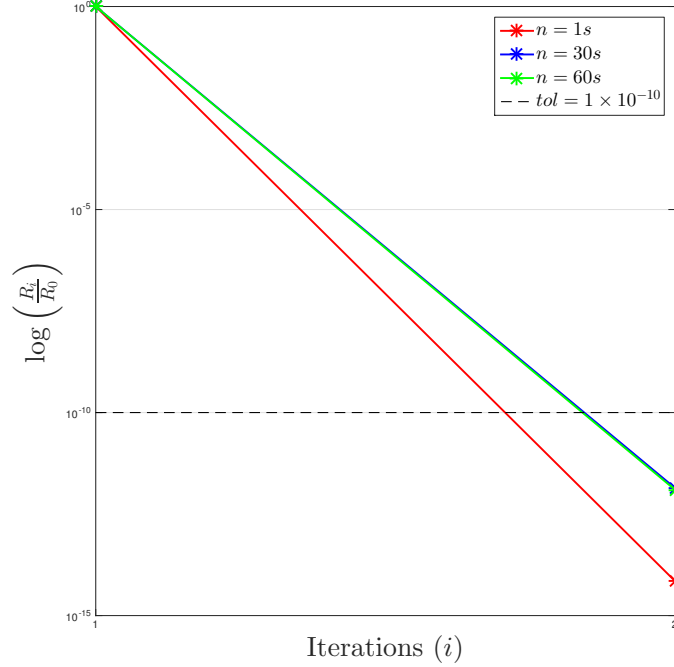
Figure 17: NR convergence at different time steps: $n = 1$ s, 30 s and 60 s, for a tolerance of 1×10^{-10} for a real seismic excitation.

7.5 Modal analysis

For the linearized problem given by expression (9), the corresponding vibrational modes that were obtained by solving the inherent eigenvalue problem are

$$
\eta_1 = \left\{ \begin{array}{c} -0.9156 \\ -0.3995 \\ -0.0449 \end{array} \right\}, \eta_2 = \left\{ \begin{array}{c} 0.1718 \\ -0.9547 \\ 0.2429 \end{array} \right\}, \eta_3 = \left\{ \begin{array}{c} 0.9903 \\ -0.1375 \\ -0.0180 \end{array} \right\} \tag{10}
$$

Figure 18 represents the vibrational mode shapes of the soil-structure system. The first mode corresponds to the lowest frequency ($f_1 = 2.6755 \, [Hz]$) and is, in terms of deformational energy, the "least expensive" of all the modes. In the same way, the second mode is also the second less "expensive" energetically speaking ($f_2 = 6.2832 \, [Hz]$). Finally, the third mode is the most "expensive", with a frequency of $f = 18.9162 \, [Hz]$.
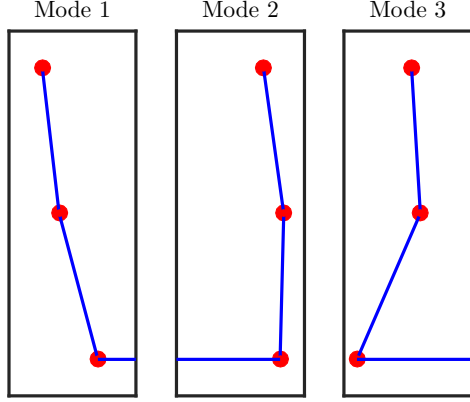
19

Figure 18: Vibrational modes representation of the proposed model.

In other words, if the soil-structure system fails it would more likely happen for the lowest frequency ($f_1 = 2.6755\,[Hz]$) and corresponding modal shape (Mode 1) (see, Figure 18). On the other hand, the system would not be likely to fail for the highest frequency ($f_3 = 18.9162\,[Hz]$, Mode 3).

Typical natural fundamental frequencies of two/three story buildings rank between $5\,[Hz]$ and $5.25\,[Hz]$. Notice that for this case the soil has been included into the model giving a fundamental frequency (f_1) of $2.6755\,[Hz]$, from which we have a drop of near the 35% with respect to the typical average values of this type of buildings ($5.25\,[Hz]$). Hence, the key importance of taking into account soil-structure interactions when it comes to dynamic analysis (even linear) of buildings. Recall, the period of vibration as the inverse of the frequency, therefore as the frequency decreases the period of vibration increases. This is exactly what occurs, as expected, including the effect of soil deformability clearly "softens" the structure increasing the period of vibration, this is not a matter of surprise as previous authors have already noticed this fact [34, 35].

8 Conclusion

We have introduced a finite difference integration of the equations of motion derived for a two-dimensional lagrangian-based model of nonlinear soil-structure interactions, i.e., large displacements and rotations. This model describes the sliding and vibrational movements of the structure when subjected to external excitations [12, 15, 36], allowing us to numerically compute the nonlinear interactions between the soil and the structure by means of a "semi-explicit" finite difference scheme.

The aforementioned approach introduces a simple but powerful tool for the study and interpretation of the vibrational/seismic behavior of civil engineering structures. Its main strength relies on the lagrangian mechanics theoretical framework used for its development, enabling us to capture the highly nonlinear (large) displacements and rotations related to both: soil and structure, as well as their interactions. Hence, we can describe not only qualitatively but also quantitatively the maximum real deformations that, in turn, lend us equivalent static forces for a suitable vibrational/seismic resistant design. It is also worth commenting on the generality of using a lagrangian framework since these kind of approaches are usually broader and less limited than their Newtonian counterparts when it comes to mathematically modelling and capturing all the physics involved in a given mechanical phenomenon.

In the same way, it is important to mention that the introduced approach can be extended to multiple degrees of freedom (MDOF), (e.g., several floors and three dimensions). However, in its current state (i.e., two dimensions), it can be used for three dimensional modelling and corresponding analysis by uncoupling the main inertial directions of the structure under study. The aim of the present work is to introduce this model and show some of its key features as well as basic ideas. However, further research is needed in order to fully understand and exploit all the novelties and aspects of the model.

Finally, four benchmark examples were tackled with this method. Here, the nonlinear motions (large deformations) of the structure were clearly "visualized" for a case in which the structure (three-story bulding) is subjected to initial conditions ("seismic excitation"), while for the example using the real acceleration record the corresponding angular rotations behave in a much linear way. A very important remark to be made is that by linearizing the proposed system and performing the modal analysis of the benchmark problems, we determined that by including the soil-structure interactions into the structural system, the fundamental natural frequency of the building is 35% lower than typical values of fundamental frequencies in buildings of similar height that have been computed without taking into account soil-structure interactions.

A Appendix

Equations (3),(4) and (5) respectively discretized. As mentioned before, the system of equations is highly nonlinear.

Discretized *Euler-Lagrange* equation for θ_1,

$$
\begin{aligned}
f_{\theta_1} =\frac{1}{2}\Big[& \Delta t^2 \sin(2\theta_{1,i+1})k_3 L_1^2 + 2\Delta t^2 \sin(2\theta_{1,i+1})k_2 L_3^2 - 2\Delta t^2 \sin(\theta_{1,i+1})gL_1 m_1 \\
& - 2g\Delta t^2 \sin(\theta_{1,i+1})L_1 m2 - \Delta t c_3 x_i + \cos(\theta_{1,i+1})L_1 m_1 x_i + 4\cos(\theta_{1,i+1})L_1 m_2 x_i \\
& - 4\cos(\theta_{1,i+1})L_1 m_1 x_{i+1} - 8\cos(\theta_{1,i+1})L_1 m_2 x_{1+1} + \Delta t c_3 x_{i+2} + 2\cos(\theta_{1,i+1})L_1 m_1 x_{i+2} \\
& + 4\cos(\theta_{1,i+1})L_1 m_2 x_{i+2} - \Delta t \cos(\theta_{1,i+1})c_3 L_1 \theta_{1,i} - 2\Delta t \cos(\theta_{1,i+1})c_2 L_3 \theta_{1,i} + 2L_1^2 m_1 \theta_{1,i} \\
& + 8L_1^2 m_2 \theta_{1,i} - 4L_1^2 m_1 \theta_{1,i+1} - 16L_1^2 m_2 \theta_{1,i+1} + \Delta t \cos(\theta_{1,i+1})c_3 L_1 \theta_{1,i+2} \\
& + 2\Delta t \cos(\theta_{1,i+1})c_2 L_3 \theta_{1,i+2} + 2L_1^2 m_1 \theta_{1,2+1} + 8L_1^2 m_2 \theta_{1,i+2} + 4\cos(\theta_{1,i+1})L_1 L_2 m_2 \theta_{2,i} \\
& + \sin(\theta_{1,i+1} - \theta_{2,i+1})L_1 L_2 m_2 \theta_{2,i}^2 - 8\cos(\theta_{1,i+1} - \theta_{2,i+1} - \theta_{2,i+1})L_1 L_2 m_2 \theta_{2,i+1} \\
& + 4\cos(\theta_{1,i+1} - \theta_{2,i+1})L_1 L_2 m_2 \theta_{2,i+2} - 2\sin(\theta_{1,i+1} - \theta_{2,i+1})L_1 L_2 m_2 \theta_{2,i}\theta_{2,i+2} \\
& + \sin(\theta_{1,i+1} - \theta_{2,i+1})L_1 L_2 m_2 \theta_{2,i+2}^2 \Big] = 0
\end{aligned}
$$

for θ_2

$$
\begin{aligned}
f_{\theta_2} =\frac{1}{2}\Big[& \Delta t^2 \sin(2\theta_{2,i+1})k_4 L_2^2 + \Delta t c_4(-x_i + x_{i+2} + 2\cos(\theta_{1,i+1})[L_1(-\theta_{1,i} + \theta_{1,i+2})]) \\
& - L_2(m_2(2g\Delta t^2 \sin(\theta_{2,i+1}) - 2\cos(\theta_{2,1+i})x_i + 4\cos(\theta_{2,i+1})x_{i+1} - 2\cos(\theta_{2,i+1})x_{i+2} \\
& - 4\cos[\theta_{1,i+1} - \theta_{2,i+1})L_1 \theta_{1,i} + \sin(\theta_{1,i+1} - \theta_{2,i+1})L_1 \theta_{1,i}^2 + 8\cos(\theta_{1,i+1} - \theta_{2,i+1}) \\
& + L_1 \theta_{1,i+1} - 4\cos(\theta_{1,i+1} - \theta_{2,i+1}) + L_1 \theta_{1,i+2} - 2\sin(\theta_{1,i+1} - \theta_{2,i+1})L_1 \theta_{1,i}\theta_{1,i+2} \\
& + \sin(\theta_{1,i+1} - \theta_{2,i+1})L_1 \theta_{1,i+2}^2) + \Delta t \cos(\theta_{2,i+1})c_4(\theta_{2,i} - \theta_{2,i+2}) \\
& + 2L_2^2 m_2(\theta_{2,i} - 2\theta_{2,i+1} + \theta_{2,i+2})\Big] = 0
\end{aligned}
$$

and for x,

$$
\begin{aligned}
f_x = \frac{1}{4}\Big[&-l_1 m_1 \theta_{1,i-1}^2 \sin(\theta_{1,i}) - 2l_1 m_2 \theta_{1,i-1}^2 \sin(\theta_{1,i}) - l_1 m_1 \theta_{1,i+1}^2 \sin(\theta_{1,i}) - 2l_1 m_2 \theta_{1,i+1}^2 \sin(\theta_{1,i}) \\
&- l_2 m_2 \theta_{2,i-1}^2 \sin(\theta_{2,i}) - l_2 m_2 \theta_{2,i+1}^2 \sin(\theta_{2,i}) + 2l_1 m_1 \theta_{1,i-1}\theta_{1,i+1} \sin(\theta_{1,i}) \\
&+ 4l_1 m_2 \theta_{1,i-1}\theta_{1,i+1} \sin(\theta_{1,i}) + 2l_2 m_2 \theta_{2,i-1}\theta_{2,i+1} \sin(\theta_{2,i}) + 4l_1 m_1 \theta_{1,i-1} \cos(\theta_{1,i}) \\
&+ 8l_1 m_2 \theta_{1,i-1} \cos(\theta_{1,i}) - 8l_1 m_1 \theta_{1,i} \cos(\theta_{1,i}) - 16l_1 m_2 \theta_{1,i} \cos(\theta_{1,i}) + 4l_1 m_1 \theta_{1,i+1} \cos(\theta_{1,i}) \\
&+ 8l_1 m_2 \theta_{1,i+1} \cos(\theta_{1,i}) + 4l_2 m_2 \theta_{2,i-1} \cos(\theta_{2,i}) - 8l_2 m_2 \theta_{2,i} \cos(\theta_{2,i}) + 4l_2 m_2 \theta_{2,i+1} \cos(\theta_{2,i}) \\
&+ 2c_1 \Delta t\, (x_{i+1} - x_{i-1}) + 4\Delta t^2 k_1 x_i + 4m_1 x_{i-1} + 4m_2 x_{i-1} - 8m_1 x_i - 8m_2 x_i + 4m_1 x_{i+1} \\
&+ 4m_2 x_{i+1} + 4m_0\,(x_{i-1} - 2x_i + x_{i+1}) \Big] = 0
\end{aligned}
$$

References

[1] Öz Yilmaz. *Seismic data analysis: Processing, inversion, and interpretation of seismic data.* Society of exploration geophysicists, 2001.

[2] Michael D Symans and Michael C Constantinou. Semi-active control systems for seismic protection of structures: a state-of-the-art review. *Engineering structures*, 21(6):469–487, 1999.

[3] Ray W Clough and Joseph Penzien. *Dynamics of structures.* Computers & Structures, Inc, 2003.

[4] Anil K Chopra. *Dynamics of structures: theory and applications to earthquake engineering.* Prentice-Hall, 2001.

[5] Robert V Whitman and Frank Edwin Richart. Design procedures for dynamically loaded foundations. 1967.

[6] Jorge A Gutierrez and Anil K Chopra. A substructure method for earthquake analysis of structures including structure-soil interaction. *Earthquake Engineering & Structural Dynamics*, 6(1):51–69, 1978.

[7] GV Narayanan and DE Beskos. Numerical operational methods for time-dependent linear problems. *International Journal for Numerical Methods in Engineering*, 18(12):1829–1854, 1982.

[8] Jacobo Bielak and Paul Christiano. On the effective seismic input for non-linear soil-structure interaction systems. *Earthquake engineering & structural dynamics*, 12(1):107–119, 1984.

[9] George Gazetas. Analysis of machine foundation vibrations: state of the art. *International Journal of Soil Dynamics and Earthquake Engineering*, 2(1):2–42, 1983.

[10] ME Agabein, RA Parmelee, and SL Lee. A model for the study of soil-structure interaction. In *Proc. 8th Conf. Int. Assoc. Bridge &Struct. Engrg., New York*, 1968.

[11] Melvin G Calkin. *Lagrangian and Hamiltonian mechanics.* World Scientific Publishing Co Inc, 1996.

[12] John P Wolf. Spring-dashpot-mass models for foundation vibrations. *Earthquake engineering & structural dynamics*, 26(9):931–949, 1997.

[13] Braja M Das. *Advanced soil mechanics*. CRC Press, 2013.

[14] John P Wolf. *Foundation vibration analysis using simple physical models*. Pearson Education, 1994.

[15] George Gazetas. Formulas and charts for impedances of surface and embedded foundations. *Journal of geotechnical engineering*, 117(9):1363–1381, 1991.

[16] José M Roesset, Robert V Whitman, and Ricardo Dobry. Modal analysis for structures with foundation interaction. *Journal of the Structural Division*, 99(3):399–416, 1973.

[17] M Pender. Earthquake-soil structure interaction, spring and dashpot models, and real soil behavior. In *Proceedings of the 3 rd South Pacific Regional Conference on Earthquake Engineering, Wellington, New Zealand*, 1983.

[18] Adel Agila, Dumitru Baleanu, Rajeh Eid, and Bulent Irfanoglu. Applications of the extended fractional euler-lagrange equations model to freely oscillating dynamical systems. *Rom. J. Phys*, 61(3-4):350–359, 2016.

[19] Razvan C Fetecau, Jerrold E Marsden, Michael Ortiz, and Matthew West. Nonsmooth lagrangian mechanics and variational collision integrators. *SIAM Journal on Applied Dynamical Systems*, 2(3):381–416, 2003.

[20] Leonard Meirovitch. *Methods of analytical dynamics*. Courier Corporation, 2010.

[21] Dennis G Zill. *Differential equations with boundary-value problems*. Nelson Education, 2016.

[22] Utku Kânoğlu and Costas Synolakis. Initial value problem solution of nonlinear shallow water-wave equations. *Physical Review Letters*, 97(14):148501, 2006.

[23] John Charles Butcher. *Numerical methods for ordinary differential equations*. John Wiley & Sons, 2016.

[24] Randall J LeVeque. *Finite difference methods for ordinary and partial differential equations: steady-state and time-dependent problems*. SIAM, 2007.

[25] Chi-Tsong Chen. *Linear system theory and design.* Oxford University Press, Inc., 1995.

[26] William F Ames. *Numerical methods for partial differential equations.* Academic press, 2014.

[27] Peter Deuflhard. *Newton Methods for Nonlinear Problems: Affine Invariance and Adaptive Algorithms.* Springer, 2004.

[28] Carl T Kelley. *Solving nonlinear equations with Newton's method.* SIAM, 2003.

[29] Dimitri P Bertsekas. *Nonlinear programming.* Athena scientific Belmont, 1999.

[30] Área de Sismología Instituto Geofísico. Observaciones del sismo del 16 de abril de 2016 de magnitud mw 7.8. intensidades y aceleraciones, 2016.

[31] Fernando José Mato Méndez. Mw7. 8 muisne, ecuador 4/16/16 earthquake observations: Geophysical clustering, intensity mapping, tsunami. 2017.

[32] Jeanne Jones, Erol Kalkan, and Christopher Stephens. Processing and review interface for strong motion data (prism) software, version 1.0. 0—methodology and automated processing. Technical report, US Geological Survey, 2017.

[33] John W Wallace, Leonardo M Massone, Patricio Bonelli, Jeff Dragovich, René Lagos, Carl Lüders, and Jack Moehle. Damage and implications for seismic design of rc structural wall buildings. *Earthquake Spectra*, 28(S1):S281–S299, 2012.

[34] Adrian S Scarlat. Effect of soil deformability on rigidity related aspects of multistory buildings analysis. *Structural Journal*, 90(2):156–162, 1993.

[35] George Mylonakis and George Gazetas. Seismic soil-structure interaction: beneficial or detrimental? *Journal of Earthquake Engineering*, 4(03):277–301, 2000.

[36] Ricardo Dobry and George Gazetas. Dynamic response of arbitrarily shaped foundations. *Journal of geotechnical engineering*, 112(2):109–135, 1986.